THE JOURNAL OF BIOLOGICAL CHEMISTRY VOL. 284, NO. 22, pp. 14875–14880, May 29, 2009


# Transmembrane Protein 16A (TMEM16A) Is a $Ca^{2+}$-regulated $Cl^-$ Secretory Channel in Mouse Airways*

Received for publication, March 12, 2009, and in revised form, March 30, 2009 Published, JBC Papers in Press, April 10, 2009, DOI 10.1074/jbc.C109.000869

**Jason R. Rock[‡], Wanda K. O'Neal[§], Sherif E. Gabriel[§], Scott H. Randell[§], Brian D. Harfe[¶], Richard C. Boucher[§], and Barbara R. Grubb[§1]**

*From the [‡]Department of Cell Biology, Duke University Medical Center, Durham, North Carolina 27708, the [§]Cystic Fibrosis/Pulmonary Research and Treatment Center, University of North Carolina, Chapel Hill, North Carolina 27599, and the [¶]Department of Molecular Genetics and Microbiology, University of Florida, Gainesville, Florida 32610*

**For almost two decades, it has been postulated that calcium-activated $Cl^-$ channels (CaCCs) play a role in airway epithelial $Cl^-$ secretion, but until recently, the molecular identity of the airway CaCC(s) was unknown. Recent studies have unequivocally identified TMEM16A as a glandular epithelial CaCC. We have studied the airway bioelectrics of neonatal mice homozygous for a null allele of *Tmem16a* (Tmem16a$^{-/-}$) to investigate the role of this channel in $Cl^-$ secretion in airway surface epithelium. When compared with wild-type tracheas, the Tmem16a$^{-/-}$ tracheas exhibited a >60% reduction in purinoceptor (UTP)-regulated CaCC activity. Other members of the *Tmem16* gene family, including *Tmem16f* and *Tmem16k*, were also detected by reverse transcription-PCR in neonatal tracheal epithelium, suggesting that other family members could be considered as contributing to the small residual UTP response. TMEM16A, however, appeared to contribute little to unstimulated $Cl^-$ secretion, whereas studies with cystic fibrosis transmembrane conductance regulator (CFTR)-deficient mice and wild-type littermates revealed that unstimulated $Cl^-$ secretion reflected ~50% CFTR activity and ~50% non-Tmem16a activity. Interestingly, the tracheas of both the Tmem16a$^{-/-}$ and the CFTR$^{-/-}$ mice exhibited similar congenital cartilaginous defects that may reflect a common $Cl^-$ secretory defect mediated by the molecularly distinct $Cl^-$ channels. Importantly, the residual CaCC activity in Tmem16a$^{-/-}$ mice appeared inadequate for normal airway hydration because Tmem16a$^{-/-}$ tracheas exhibited significant, neonatal, lumenal mucus accumulation. Our data suggest that TMEM16A CaCC-mediated $Cl^-$ secretion appears to be necessary for normal airway surface liquid homeostasis.**

The disease cystic fibrosis (CF)[2] occurs due to the loss of the epithelial cAMP-mediated $Cl^-$ channel CFTR. The calcium-activated $Cl^-$ conductance (CaCC) channel has often been referred to as the "alternate" $Cl^-$ channel (1) because it may serve to protect tissues that lack CFTR by providing a parallel route for $Cl^-$ secretion across the apical membrane. Thus, identification and characterization of CaCC and the gene that encodes this activity has become of critical importance to identify a possible therapeutic target for CF disease. Despite the important contribution of CaCC in regulated ion and fluid transport of the airway, this function has not until recently been assigned to a known gene.

The anoctamin/TMEM16 family of genes has been proposed to encode CaCC proteins (2–4). Three independent laboratories identified TMEM16A, also known as Ano1, as a CaCC and suggested a role for TMEM16A in glandular (mammary, salivary) secretion. Yang *et al.* (4) used a bioinformatic approach to identify *TMEM16A* and then confirmed CaCC function by expression cloning in HEK293 cells and small interfering RNA knockdown in mouse salivary glands. Caputo *et al.* (2) utilized the observation that chronic interleukin-4 stimulation of airway epithelial cells resulted in increased CaCC activity to identify *TMEM16A* by microarray analysis and demonstrated that TMEM16A also showed an ion channel activation, inhibition, and anion selectivity profile consistent with native airway CaCCs. Lastly, Schroeder *et al.* (3) used an elegant expression cloning approach to identify the *Xenopus* ortholog of *TMEM16A* and characterize its function and expression, *i.e.* in glands (mammary, salivary). Collectively, *TMEM16A* clearly demonstrates many if not all of the characteristics required of a candidate gene to produce airway epithelial CaCC. Interestingly, mice that lack *Tmem16a* (Tmem16a$^{-/-}$) were generated prior to identification of TMEM16A function. These mice demonstrated failure to thrive, died shortly after birth, and exhibited a severe malformation of the tracheal cartilage rings (5).

In contrast to glands, superficial airway epithelial cells finely balance transepithelial ion transport to maintain the thin layer of liquid on airway surfaces essential for mucociliary clearance (MCC) (6). This balance is achieved via the opposing activities of the epithelial $Na^+$ channel (ENaC), primarily responsible for $Na^+$ absorption (and osmotically coupled liquid absorption) *versus* at least two apical membrane $Cl^-$ channels, CFTR (responsive to cAMP signaling) and CaCC, responsible for $Ca^{2+}$ mediated $Cl^-$ secretion. The identification of TMEM16A as mediating CaCC activity now provides an opportunity to better understand the fine tuning that produces appropriate airway surface liquid (ASL) volume and MCC.

In the present study, we utilized tracheas resected from newborn Tmem16a$^{-/-}$, $^{+/-}$, and wild-type (WT) mice to investi-

* This work was supported, in whole or in part, by National Institutes of Health Grants P30 Dk065988, P01-HL034322, and SCCOR NIH 5 P50 HL084934. This work was also supported by RDP Grant CFF R0 26-CR037 from the Cystic Fibrosis Foundation.

[1] To whom correspondence should be addressed: Cystic Fibrosis/Pulmonary Research and Treatment Center, 7011 Thurston-Bowles Bldg., CB# 7248, the University of North Carolina, Chapel Hill, NC 27599. Tel.: 919-966-5602; E-mail: bgrubb@med.unc.edu.

[2] The abbreviations used are: CF, cystic fibrosis; CFTR, cystic fibrosis transmembrane conductance regulator; TMEM, transmembrane protein; CaCC, calcium-activated $Cl^-$ channels; ENaC, epithelial $Na^+$ channel; MCC, mucociliary clearance; ASL, airway surface liquid; WT, wild type; RT-PCR, reverse transcription-PCR; AB-PAS, Alcian blue periodic acid Schiff.

gate the contribution of TMEM16A to unstimulated and $Ca^{2+}$-regulated $Cl^-$ secretion. Regions of tracheas devoid of submucosal glands were selected for study to characterize the role of TMEM16A in superficial epithelial $Cl^-$ secretion. Because tracheas from Tmem16a$^{-/-}$ mice exhibited some residual CaCC activity, mRNA analysis was performed to identify other TMEM family members that might function as CaCCs in the neonatal trachea. We also compared the tracheal bioelectric properties of neonatal CF tracheas with those of Tmem16a$^{-/-}$ tracheas to elucidate the relative roles of each $Cl^-$ channel in airway $Cl^-$ secretion and mucus clearance. Finally, we compared the histology and morphology of the tracheas from Tmem16a$^{-/-}$ and Cftr$^{-/-}$ mice in an attempt to link defective $Cl^-$ secretion to tracheal cartilaginous defects and the mode of early postnatal death characteristic of these animals.

## EXPERIMENTAL PROCEDURES

*Tracheal Bioelectric Properties*—All pups were removed from their mothers within 12–48 h after birth and studied immediately. Both gene mutations (*Tmem16a*; see Ref. 5 for details) and *Cftr* (*cftr*$^{tm1unc}$) were on a mixed strain background. There was no significant difference in the body mass among the three genotypes of the Tmem16a mice or the Cftr$^{-/-}$ (CF) mice and their WT littermates at this early age (data not shown). For the CF line, pups $^{+/-}$ for CFTR are considered to be WT because we have not detected phenotypic differences in airway bioelectric properties between tracheas $^{+/+}$ *versus* $^{+/-}$ for CFTR (data not shown). The pups for the Ussing chamber study were killed by an overdose of ketamine/xylazine, and the tracheas were immediately removed, mounted on an Ussing chamber, and studied. All preparations were bathed bilaterally in Krebs bicarbonate ringer, as reported previously (7). The non-stimulated short circuit current ($I_{sc}$) was measured when the $I_{sc}$ stabilized (~30 min after mounting). The tracheas were then exposed cumulatively to a $Na^+$ transport blocker (amiloride, $10^{-4}$ M, lumenal), UTP ($10^{-4}$ M, lumenal), forskolin ($10^{-5}$ M, lumenal), and a blocker of $Cl^-$ secretion (bumetanide, $10^{-4}$ M, basolateral), and bioelectric properties were measured after each drug addition. The investigators conducting the experiments and calculating the data were blinded as to genotype. Animals were routinely genotyped by PCR using tail DNA collected when the pups were euthanized. Genotyping was as described (5).

*RNA Isolation*—For isolation of tracheal epithelial RNA, 3–4 wild-type (ICR strain) newborn mice were euthanized by decapitation, and tracheas were dissected in ice-cold phosphate-buffered saline. Tracheas were cut into halves at the level of the sixth cartilage ring to obtain distal and proximal halves and incubated in 10 units/ml Dispase (BD Biosciences, San Jose, CA) for 25 min at room temperature. The epithelium was peeled from the mesenchyme using fine forceps. Epithelia and mesenchyme from proximal and distal trachea were collected in phosphate-buffered saline on ice before quick freezing in liquid nitrogen and storage at −80 °C until RNA isolation. RNA was isolated according to the manufacturer's specifications using either the RNeasy kit (for adult trachea/brain/eye) or the RNeasy Plus kit (for newborn epithelium/mesenchyme) (Qiagen, Germantown, MD). Other RNA samples (adult lung) were purchased from Ambion. RNA was analyzed for concentration and quality on the NanoDrop spectrophotometer and Agilent 2100 bioanalyzer. 200 ng of total RNA was used to synthesize cDNA using SuperScript III reverse transcriptase and the manufacturer's protocol (Invitrogen). For adult samples, 100 ng of cDNA was used in each PCR reaction; 200 ng was used for newborn tracheal samples. Primers were ordered specifically to cross introns and are as follows (accession numbers used are given in parentheses): *Tmem16a* (NM_178642), forward, 5′-GGCTTTGTCACCCTGTTTGT-3′, reverse, 5′-GAGAGCGTGTGATTGACGAA-3′; *Tmem16b* (NM_153589), forward, 5′-GGCAAGTTCTCCGTCATCAT-3′, reverse, 5′-AACCTCCTGGTCGAACTGTG-3′; *Tmem16f* (NM_175344), forward, 5′-ATGGGACACCGTTGAGCTAC-3′, reverse, 5′-TCAGGTACTTCTGGATCGGG-3′; *Tmem16j* (NM_178381), forward, 5′-TGAAGGATGGGGTTTTTGAG-3′, reverse, 5′-CCAAGAGGGCACATGAAGAT-3′; *Tmem16k* (NM_133979), forward, 5′-TGCAGTTTGGCTATGTGAGC-3′, reverse, 5′-GGCCAGTTTCTGTTGGATGT-3′. For RT-PCR, ImmoMix (Bioline, Taunton, MA) was used according to recommended conditions with a 25-$\mu$l volume in an ABI thermocycler. Cycling conditions were as follows: 95 °C for 10 min hot start followed by 35 cycles of 95° 30 s, 55 °C for 30 s, 72° for 30 s, ending with 7 min at 72 °C and a 4 °C hold. All RT-PCR reactions included no reverse-transcriptase controls, which were negative (not shown), and all products were cloned from positive control tissues and sequenced to confirm product identity.

*Histology*—Preparations removed from Ussing chambers were fixed to examine histologically for the presence of submucosal glands. After removal from the chambers, these small specimens were stained with tissue marking dye (Triange Biomedical Sciences) for easy visualization and then processed. For general histology, tracheas from newborn mouse pups, euthanized by an overdose of ketamine/xylazine, were fixed *in situ* in neutral buffered formalin, processed, and stained with Alcian blue periodic acid Schiff (AB-PAS) or hematoxylin and eosin. For histology of the CF tracheas, we utilized ΔF508 CF pups (*cftr*$^{tm1kth}$). Note that the histological defects and bioelectrics of the two CFTR mutations appear identical (8).[3]

*Statistics*—When more than two groups were compared (Tmem16a mice), a one-way analysis of variance was used. When only two groups were being compared (CF *versus* WT), a Student's *t* test was used. Data are shown as means ± S.E.

## RESULTS

The tracheal bioelectric properties of newborn mice, homozygous for a null allele of *Tmem16a* (referred to as Tmem16a$^{-/-}$ in this study), and their wild-type ($^{+/+}$) and heterozygous ($^{+/-}$) littermates are shown in Fig. 1*A*. There was no significant difference in the unstimulated short circuit current ($I_{sc}$), the response to amiloride, or the residual (post-amiloride) $I_{sc}$ among the three genotypes. However, a one-way analysis of variance revealed that the response to UTP differed significantly (**, $p \leq 0.01$) among the three groups. Although the magnitude of the UTP response in the

[3] B. R. Grubb, personal communication.

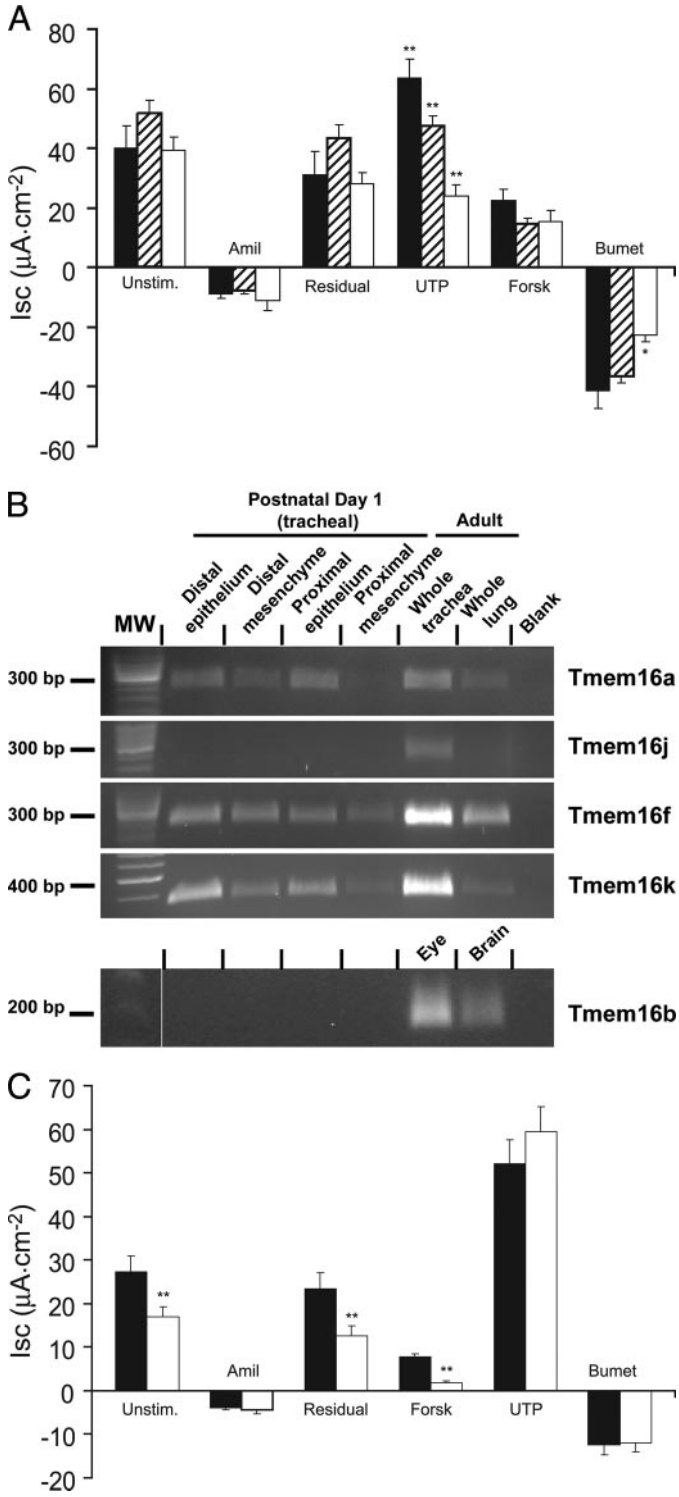


FIGURE 1. **Bioelectric and expession patterns of TMEMs and CFTR neonatal tracheas.** *A*, tracheal bioelectrics of WT (*solid bars*, $n = 7$), Tmem16a$^{+/-}$ (*hatched bars*, $n = 28$), and Tmem16a$^{-/-}$ pups (*open bars*, $n = 7$). *Unstim.* indicates the unstimulated $I_{sc}$ before drug application. Then, amiloride (*Amil*) $10^{-4}$ M was added apically, and the magnitude of the resulting change is shown. The residual $I_{sc}$ is the $I_{sc}$ remaining after amiloride application. Then, UTP (UTP $10^{-4}$) was added apically followed by apical forskolin (*Forsk*) $10^{-5}$ M, and then bumetanide $10^{-4}$ (*Bumet*) was added basolaterally. The UTP response differed (**, $p \leq 0.01$) from the other two groups, *, $p \leq 0.05$ *versus* $^{+/+}$ and $^{+/-}$. Data are means ± S.E. (*error bars*). *B*, expression of mRNA from TMEM isoforms in epithelium and mesenchyme isolated from trachea at postnatal day 1. Tracheae were separated into sections, RNA was isolated, and RT-PCR was performed as described under "Experimental Procedures." Whole adult trachea and lung were used as positive controls for *Tmem16 a*, *Tmem16f*, *Tmem16j*, and *Tmem16k*. For *Tmem16b*, mouse eye and brain were used because *Tmem16b* was not detected in adult trachea or lung (not shown). *Blank* = water control; *MW* = molecular weight marker. Approximate sizes of products are given (in bp). *C*, tracheal bioelectrics of WT (*solid bars*, $n = 29$) and CF (*open bars*, $n = 31$) pups. Drug additions and symbols are the same as in *panel A*, with the exception that forskolin was added before UTP. **, $p \leq 0.01$ from WT. Data are means ± S.E (*error bars*).

Tmem16a$^{-/-}$ tracheas was significantly reduced when compared with the other two groups, it should be noted that a significant residual UTP response still remained in the Tmem16a$^{-/-}$ tracheas. The response to forskolin did not differ among the three genotypes, but the response to bumetanide was significantly reduced in the Tmem16a$^{-/-}$ tracheas when compared with the other two genotypes.

We considered whether the measured bioelectric signals could have originated in the murine submucosal glands. However, because no submucosal glands were identified in any tracheal sections examined histologically (18 sections from 9 individual tracheas; data not shown) after removal of the tissue from the Ussing chambers, we concluded that the signal must originate from the epithelium lining the tracheal lumen.

In an effort to develop a comprehensive understanding of the proteins involved in the residual UTP-activated response, mRNA analyses for other TMEM family members in neonatal tracheal epithelium were conducted (Fig. 1*B*). Of the TMEM isoforms carefully evaluated to date, mRNA from *Tmem16a, Tmem16f,* and *Tmem16k* were shown to be expressed in both proximal and distal tracheal epithelium and mesenchyme. Thus, these members are candidates for the residual CaCC activity seen in the Tmem16a$^{-/-}$ mice. Other family members, including *Tmem16b* and *Tmem16j*, were not detected in neonatal tissue, although *Tmem16j* was clearly detected in adult mouse trachea.

The tracheal bioelectric properties of newborn WT and CF pups are shown in Fig. 1*C*. The unstimulated $I_{sc}$ was significantly reduced in the CF tracheas when compared with WT tracheas (**, $p \leq 0.01$), whereas the amiloride response did not differ between the two genotypes. The post-amiloride residual $I_{sc}$ was also significantly reduced in the CF tracheas (**, $p \leq 0.01$), likely reflecting the reduced unstimulated $I_{sc}$ in these preparations. The forskolin response in CF tracheas was significantly reduced (**, $p \leq 0.01$) when compared with WT. The response to UTP and bumetanide did not differ between the genotypes.

Both the Tmem16a$^{-/-}$ and the CF tracheas (Fig. 2, *B* and *F*) exhibited anatomical defects in the cartilaginous rings that appeared similar, with reduced tracheal size when compared with WT (Fig. 2, *A* and *E*). In mice (both Tmem16a$^{-/-}$ and CF), the cartilaginous rings on the ventral surface were discontinuous, and the epithelial layer exhibited evaginations. However, the defect was more extensive in the Tmem16a$^{-/-}$ tracheas, extending the entire length of the trachea, whereas in the CF tracheas, it tended to be confined to the first 3–4 tracheal rings. There was significant mucus (red-stained neutral mucopolysaccharide) accumulation in the lumen of the Tmem16a$^{-/-}$ tracheas, which nearly plugged the trachea in some animals (Fig. 2*D*). Most of the mucus was in the lower two-thirds of the

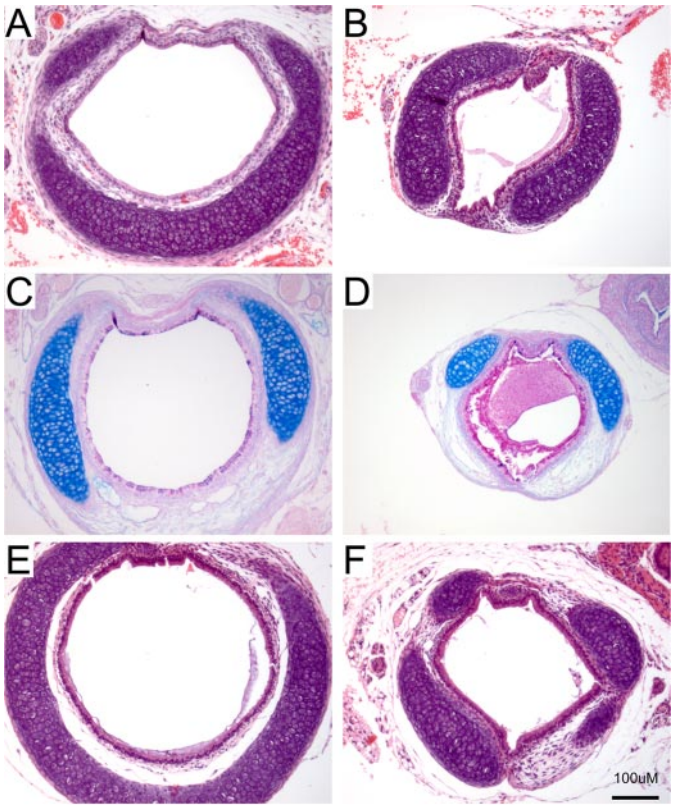


FIGURE 2. **Histology of WT and mutant tracheas (*A*, *B*, *E*, and *F* are stained with hematoxylin and eosin, and *C* and *D* are stained with AB-PAS).** *A*, WT (littermate to *B*). In the normal trachea, the cartilage is continuous except along the posterior membrane (at the *top* of the figure), giving the normal trachea a rounded appearance (see also *C* and *E*). Due to the plane of section, the cartilage can appear discontinuous in the WT tissue (as in *C*). *B*, Tmem16a$^{-/-}$ trachea exhibiting cartilaginous defects on the ventral (*bottom* of figure) side. Evaginations of the epithelial layer are evident, and the normal rounded appearance of the lumen is lost. *C*, WT trachea stained with AB-PAS. *D*, Tmem16a$^{-/-}$ trachea stained with AB-PAS exhibiting significant lumenal mucus accumulation. *E*, trachea of WT (littermate to F). *F*, CF trachea exhibits a cartilaginous defect on the ventral side that results in discontinuous cartilaginous rings. Epithelial evaginations are also evident. All were photographed at same magnification; see scale in *F*.

trachea, with little in the mainstem bronchi. The smaller airways were devoid of mucus. The CF tracheas did not contain any mucus.

## DISCUSSION

CaCCs have been implicated in a variety of physiological functions, including fluid secretion, olfactory transduction (9–11), and smooth muscle contraction (12). However, until recently, the molecular identity of these channels has eluded identification. TMEM16A has now been convincingly identified as a calcium-activated $Cl^-$ channel (or a subunit thereof) with a unique structure but no obvious $Ca^{2+}$ binding sites (3).

A CaCC dominates the $Cl^-$ secretory response of the murine trachea, and we have previously speculated that this $Cl^-$ conductance protects the CF mouse from CF-like airway disease (1, 13). CaCC has also been demonstrated to be an important functional $Cl^-$ channel in CF human airway epithelia when CFTR, the cAMP-mediated $Cl^-$ channel, is non-functional (14–16).

Gene expression data indicate that the TMEM16A is expressed at high levels in exocrine glands and in organs rich in glands (2). In the mouse *in vivo*, it has been shown that Tmem16A mediates muscarinic regulated salivary flow, as intravenous treatment of mice with *Tmem16a* small interfering RNA significantly reduced Tmem16A expression and pilocarpine-stimulated salivary flow in submandibular glands (4).

In the present investigation, we studied the function of Tmem16A in the airways of neonatal pups in which the *Tmem16a* gene was deleted (5) and compared these data with both WT and *Cftr* gene targeted mice. The unstimulated $I_{sc}$ reflects components of electrogenic $Na^+$ absorption and $Cl^-$ secretion, and this parameter did not differ among the three Tmem16a genotypes ($^{+/+}$, $^{+/-}$, $^{-/-}$). The amiloride-sensitive electrogenic $Na^+$ absorption also did not differ among the three genotypes, nor was the amiloride-insensitive residual current, an index of unstimulated $Cl^-$ secretion, different between the three genotypes. Thus, we conclude that Tmem16A does not contribute to unstimulated $Cl^-$ secretion, nor does it exhibit a regulatory relationship to ENaC, as proposed for CFTR (17).

As a probe of regulated $Cl^-$ secretion in neonatal Tmem16a$^{-/-}$ tracheal preparations, UTP was used as an agonist to increase intracellular calcium, which, in amiloride-pretreated tissues, predominantly activates CaCC. We observed a significant *Tmem16a* gene dose effect on the magnitude of the UTP response (Fig. 1*A*), with Tmem16a$^{-/-}$ tracheas exhibiting a significantly reduced (~60%) response when compared with the WT tissue. However, because a significant UTP response persisted in the Tmem16a$^{-/-}$ tracheas, it is likely that a genetically distinct CaCC also plays a role in the $Cl^-$ secretory response of this tissue. A role for Bestrophin 2 in contributing to CaCC in the murine airway has been suggested by RNA inhibition studies in primary mouse tracheal cells (18). By reducing Best2 mRNA levels, the authors report a significant reduction in ATP-stimulated currents to ~50% of wild-type levels. In our study, the magnitude of the forskolin-induced $Cl^-$ secretory responses did not differ among the three genotypes, suggesting that TMEM16A is not cAMP-regulated. Finally, the response to bumetanide (which blocks basolateral $Cl^-$ entry and thus $Cl^-$ secretion) was attenuated in the Tmem16a$^{-/-}$ tracheas proportionate to the magnitude of the UTP responses in these tissues.

For CaCC to have its postulated protective role in the CF mouse lung (1), it must be expressed in the superficial epithelium. Immunohistochemical analysis (4) suggested surface expression in distal airway epithelium. Our histologic analyses of the region of the excised neonatal tracheas assayed in Ussing chambers revealed a well differentiated superficial epithelium with an absence of glands. Molecular analyses confirmed that *Tmem16a* was expressed in this epithelium (Fig. 2*B*). Thus, these studies are the first to assign a molecular identity to a CaCC expressed in murine superficial airway epithelia.

There are several possible candidate CaCCs that mediate the residual UTP-regulated activity in Tmem16a$^{-/-}$ mice. For example, there are 10 identified genes in the *TMEM* gene family in mice and humans, but CaCC function has only been ascribed to *Tmem16a* and *Tmem16h*. Because the Tmem16a$^{-/-}$ mice exhibit residual UTP- ($Ca^{2+}$-) stimulated $Cl^-$ secretion, levels of mRNA expression of other *TMEM* gene family members were measured in neonatal tracheas (Fig. 2*B*). *Tmem16f* and *Tmem16k*, but not *Tmem16b* or *Tmem16j*, were detected.

Alternatively, future studies are required to assign residual CaCC function to the protein products of *TMEM* gene family members or other genes.

As one approach to determine the relative roles of TMEM16A *versus* CFTR in neonatal tracheal $Cl^-$ secretion, we studied CF mouse tracheas also excised 12–24 h after birth. The neonatal CF tracheas exhibited a significant reduction in the unstimulated $I_{sc}$ when compared with WT, suggesting that a portion of this $Cl^-$ secretion is mediated via CFTR (~50%). As reported for adult CF mice (13), there was no difference in the amiloride response between the two genotypes. Unlike the Tmem16a$^{-/-}$ tracheas, the tracheas from the CF pups exhibited a significant decrease in the post-amiloride residual $I_{sc}$, supporting the notion that the post-amiloride residual $I_{sc}$ reflects $Cl^-$ secretion. Note that because a significant post-amiloride $I_{sc}$ remained in the CF tracheas, it is possible that a CaCC (but probably not TMEM16A, as this residual $I_{sc}$ is not reduced in Tmem16a$^{-/-}$ mice) is responsible for the residual $I_{sc}$. With respect to regulated $Cl^-$ secretion, the pattern in the CF mouse was the inverse of the TMEM16A mutant mouse, *i.e.* forskolin-stimulated $I_{sc}$ was small in WT mice but reduced more than 75% in CF mice, whereas UTP-stimulated $Cl^-$ secretion was large and unaffected by *CFTR* gene targeting. Note that in the adult CF mouse, there is no defect in either the unstimulated $I_{sc}$ or the residual $I_{sc}$, suggesting that CFTR function wanes with age (13).

Interestingly, in mice in which either the cAMP-mediated $Cl^-$ channel (*Cftr* gene) or the calcium-mediated $Cl^-$ channel (*Tmem16a* gene) was deleted, a similar congenital defect in the tracheal cartilage was observed (5, 8, 19). In mice with either mutation, this defect involves the cartilaginous rings on the ventral surface of the trachea. In the Tmem16a$^{-/-}$ pups, the cartilaginous rings were discontinuous along the entire length of the trachea. This phenotype, which extends into the mainstem bronchi, was 100% penetrant in the Tmem16a mutant pups (5). This cartilaginous defect was also present in both the CFTR null mutation (*cftr*$^{tm1unc}$) and the ΔF 508 CFTR mutations (*cftr*$^{tm1kth}$) at a frequency of occurrence ranging from 86 to 100% (8). However, in the *cftr*$^{tm1unc}$ mutation, the defect was confined to the upper trachea, whereas in the *cftr*$^{tm1kth}$ mice, the defect was present all along the trachea (8). Because the two CF mouse models studied were on different genetic backgrounds, the difference in phenotypic expression of the tracheal malformation may be a strain-dependent phenomenon (8).

Two quite different hypotheses may describe the molecular mechanisms producing the similar morphologic findings in mice with different genetic mutations. First, it is possible that both CFTR and TMEM16A expression in mesenchymal structures, *e.g.* tracheal smooth muscle, are important for cartilage development. Both CFTR (20) and TMEM16A (5) have been reported to be expressed in tracheal smooth muscle, and we observed expression of TMEM16A in the mesenchyme isolated from neonatal tracheal tissue (Fig. 1*B*). Second, it is possible that the defects reflect a reduction in $Cl^-$ (and liquid) secretion into the fetal lung. A reduction in both basal (CFTR) and $Ca^{2+}$-regulated (TMEM16A) $Cl^-$ secretion is predicted to reduce fetal lung liquid secretion and decrease pulmonary transmural pressure gradients. Transmural pressure gradients are important stimuli for lung growth, perhaps including tracheal cartilage.

The presence of mucus (neutral mucopolysaccharide red-stained material in AB-PAS-stained sections) in the lumen of the Tmem16a$^{-/-}$ tracheas was striking and not previously reported by Rock *et al.* (5), possibly due to differences in fixation techniques. A similar accumulation of mucus in the trachea has been observed in a mouse model of ASL depletion caused by transgenic overexpression of βENaC (21). Based on this comparison, we speculate that the mucus accumulation reflects a defect in CaCC-mediated $Cl^-$ secretion and consequent ASL depletion.

However, no mucus was observed in the CF tracheas. Although the CF neonatal tracheas exhibit a reduction in the unstimulated secretion by ~50% and a greater than 75% reduction in the cAMP-stimulated response, the absolute magnitudes of these reductions in $Cl^-$ secretion were small (10 and 6 $\mu A \cdot cm^{-2}$, respectively), likely too small to reduce ASL volume and produce a reduction in mucus clearance sufficient to produce mucus accumulation. In contrast, in the Tmem16a$^{-/-}$ tracheas, the basal $Cl^-$ secretory rate appeared normal, but the reduction in stimulated $Cl^-$ secretion via CaCC (TMEM16A) was large (~40 $\mu A \cdot cm^{-2}$). We speculate that it is the large, regulated component of $Cl^-$ secretion that is necessary to maintain ASL hydration sufficient for adequate MCC in murine airways.

The identification of both cartilaginous defects and intralumenal mucus accumulation have led us to re-evaluate the mode of early death of Tmem16a$^{-/-}$ mice (5). The cartilaginous defects were extensive in the Tmem16a$^{-/-}$ tracheas and produced increased compliance that resulted in collapse of Tmem16a$^{-/-}$ tracheas with the slightest pressure. Morphometric indications of this "floppiness" were noted in the fixed tracheas of Tmem16a$^{-/-}$ mice (Fig. 2*B*). We speculate that pressure-induced collapse of tracheas caused intralumenal mucus-mediated adhesion of opposing tracheal walls to occur, resulting in acute asphyxia in most neonates (90% of the pups die by day 9 (5)). The reported presence of air in the esophagus and stomach (5) likely is a result of gasping secondary to asphyxia.

In conclusion, we have shown that *Tmem16a* encodes for the dominant CaCC activity in the superficial epithelium of neonatal murine airways. Based on the accumulation of mucus in airways likely due to deficient $Cl^-$ and liquid secretion, and perhaps the relative magnitude of the cartilaginous defects in Tmem16a$^{-/-}$ tracheas, TMEM16A, not CFTR, appears to be the dominant $Cl^-$ channel in mouse airways. We speculate that maneuvers to extend the life of Tmem16a$^{-/-}$ mice and/or generation of airway-specific *Tmem16a* conditional null mice will produce a mouse lung model of CF-like defective $Cl^-$ and liquid secretion, intrapulmonary mucus stasis, inflammation, and death.

*Acknowledgments—We thank T. D. Rogers and Kim Burns (University of North Carolina (UNC) CF Center Histology Core) and Kristy Terrell and Rodney Gilmore (UNC CF Center Molecular Biology Core) for their excellent technical assistance.*

## REFERENCES


1. Clarke, L. L., Grubb, B. R., Yankaskas, J. R., Cotton, C. U., McKenzie, A., and Boucher, R. C. (1994) *Proc. Natl. Acad. Sci. U. S. A.* **91,** 479–483
2. Caputo, A., Caci, E., Ferrera, L., Pedemonte, N., Barsanti, C., Sondo, E., Pfeffer, U., Ravazzolo, R., Zegarra-Moran, O., and Galietta, L. J. (2008) *Science* **322,** 590–594
3. Schroeder, B. C., Cheng, T., Jan, Y. N., and Jan, L. Y. (2008) *Cell* **134,** 1019–1029
4. Yang, Y. D., Cho, H., Koo, J. Y., Tak, M. H., Cho, Y., Shim, W. S., Park, S. P., Lee, J., Lee, B., Kim, B. M., Raouf, R., Shin, Y. K., and Oh, U. (2008) *Nature* **455,** 1210–1215
5. Rock, J. R., Futtner, C. R., and Harfe, B. D. (2008) *Dev. Biol.* **321,** 141–149
6. Tarran, R., Button, B., and Boucher, R. C. (2006) *Annu. Rev. Physiol.* **68,** 543–561
7. Grubb, B. R. (2002) *Methods Mol. Med.* **70,** 525–535
8. Bonvin, E., Le Rouzic, P., Bernaudin, J. F., Cottart, C. H., Vandebrouck, C., Crié, A., Leal, T., Clement, A., and Bonora, M. (2008) *J. Physiol.* **586,** 3231–3243
9. Tarran, R., Loewen, M. E., Paradiso, A. M., Olsen, J. C., Gray, M. A., Argent, B. E., Boucher, R. C., and Gabriel, S. E. (2002) *J. Gen. Physiol.* **120,** 407–418
10. Kunzelmann, K., Milenkovic, V. M., Spitzner, M., Soria, R. B., and Schreiber, R. (2007) *Pfluegers Arch. Eur. J. Physiol.* **454,** 879–889
11. Matthews, H. R., and Reisert, J. (2003) *Curr. Opin. Neurobiol.* **13,** 469–475
12. Angermann, J. E., Sanguinetti, A. R., Kenyon, J. L., Leblanc, N., and Greenwood, I. A. (2006) *J. Gen. Physiol.* **128,** 73–87
13. Grubb, B. R., Paradiso, A. M., and Boucher, R. C. (1994) *Am. J. Physiol. Cell Physiol.* **267,** C293–300
14. Knowles, M. R., Clarke, L. L., and Boucher, R. C. (1991) *N. Engl. J. Med.* **325,** 533–538
15. Mason, S. J., Paradiso, A. M., and Boucher, R. C. (1991) *Br. J. Pharmacol.* **103,** 1649–1656
16. Stutts, M. J., Chinet, T. C., Mason, S. J., Fullton, J. M., Clarke, L. L., and Boucher, R. C. (1992) *Proc. Natl. Acad. Sci. U. S. A.* **89,** 1621–1625
17. Stutts, M. J., Canessa, C. M., Olsen, J. C., Hamrick, M., Cohn, J. A., Rossier, B. C., and Boucher, R. C. (1995) *Science* **269,** 847–850
18. Barro-Soria, R., Schreiber, R., and Kunzelmann, K. (2008) *Biochim. Biophys. Acta* **1783,** 1993–2000
19. Grubb, B. R., Livraghi, A., Rogers, T. D., Wilkinson, K. J., Hudson, E. J., Boucher, R. C., and O'Neal, W. K. (2007) *Pediatr. Pulmonol. Suppl.* **30,** 280–281
20. Vandebrouck, C., Melin, P., Norez, C., Robert, R., Guibert, C., Mettey, Y., and Becq, F. (2006) *Respir. Res.* **7,** 113
21. Mall, M., Grubb, B. R., Harkema, J. R., O'Neal, W. K., and Boucher, R. C. (2004) *Nat. Med.* **10,** 487–493